

Using Effective Connectivity Measures and Stacked Autoencoder for Diagnosing Autism Spectrum Disorder by Resting-State fMRI Data

Pegah Navaei¹, Ali Khadem^{1*} , Effat Jalaeian Zaferani²

¹ Department of Biomedical Engineering, Faculty of Electrical Engineering, K. N. Toosi University of Technology, Tehran, Iran

² Faculty of Computer Engineering, K. N. Toosi University of Technology, Tehran, Iran

*Corresponding Author: Ali Khadem

Received: 08 January 2024 / Accepted: 08 September 2024

Email: alikhadem@kntu.ac.ir

Abstract

Purpose: The objective of this paper is to study the feasibility of using effective connectivity (Granger Causality) (GC) obtained from resting-state functional Magnetic Resonance Imaging (rs-fMRI) data and stacked autoencoder for diagnosing Autism Spectrum Disorder (ASD) and comparing the results with those obtained using functional connectivity (Pearson Correlation Coefficient) (PCC). ASD affects the normal development of the brain in the field of social interactions and communication skills. Because diagnosing ASD using behavioral symptoms is a time-consuming subjective process that needs the exact collaboration of the ASD subject or his/her relatives, in recent years diagnosing ASD using resting-state functional neuroimaging modalities like rs-fMRI, has been taken into consideration.

Materials and Methods: We used rs-fMRI data and compared the use of functional and effective connectivity features using an autoencoder to classify people with ASD from healthy subjects. We used ABIDE dataset and divided the brain into 100 regions using the Harvard-Oxford (HO) Atlas. We calculated the PCC in classification using functional connectivity, and we calculated the GC in classification using effective connectivity. We used a stacked autoencoder to reduce the dimension of feature-space and a multi-layered perceptron (MLP) neural network as a classifier in both classifications.

Results: We achieved an accuracy of 67.8%, a sensitivity of 68.5%, and a specificity of 66.6% in classification using functional connectivity, and we achieved an accuracy of 67.6%, a sensitivity of 73.1%, and a specificity of 60.8% in classification using effective connectivity.

Conclusion: Although the accuracy obtained using functional and effective connectivity are almost similar, the sensitivity is notably higher using effective connectivity. Since sensitivity is more important than specificity in the medical diagnosis, it seems that using effective connectivity features may outperform the ASD diagnosis in practice. The purpose of this paper is to diagnose ASD using effective connectivity measures and deep neural networks by rs-fMRI data, but we compare its results with functional connectivity measures. As far as we know, this is the first time that Granger Causality (GC) and stacked autoencoder have been used to diagnose ASD together.

Keywords: Autism Spectrum Disorder; Resting-State functional Magnetic Resonance Imaging; Functional and Effective Brain Connectivity; Pearson Correlation Coefficient; Granger Causality; Stacked Autoencoder.

1. Introduction

Autism Spectrum Disorder (ASD) disrupts the normal development of the brain in terms of social interactions and communication skills [1]. A comprehensive systematic review and meta-analysis of 74 articles published from 2008 to 2021 reported the high global prevalence of ASD. The prevalence of ASD in the world is reported to be 0.6% (95% confidence interval: 0.4–1%). Subgroup analyses indicated that the prevalence of ASD in Asia, America, Europe, Africa, and Australia was 0.4% (95% CI: 0.1–1), 1% (95% CI: 0.8–1.1), 0.5% (95% CI: 0.2–1), 1% (95% CI: 0.3–3.1), 1.7% (95% CI: 0.5–6.1), respectively [2]. The current diagnosis of ASD is mainly based on an assessment of a person’s social interactions, communication, and behavioral characteristics. A recent hypothesis suggests that the abnormal condition in people with ASD is due to impaired connections between brain regions, which ultimately affects the global network of the brain; therefore, in recent years, functional neuroimaging techniques have been used to study and diagnose ASD. Among them, functional Magnetic Resonance Imaging (fMRI) has been widely used to assess the functional network of the brain [3]. There are generally two types of fMRI data. The first type is resting-state fMRI (rs-fMRI) data, and the second type is called task-based fMRI in which a person is required to perform a specific mental or physical activity during imaging. Rs-fMRI data compared with task-based fMRI data is preferable for children or patients who may not collaborate properly in performing the required tasks. Various studies also show that the Signal-to-Noise Ratio (SNR) of rs-fMRI data is better than that of task-based data [4]. Since people with ASD find it difficult to collaborate on acquiring task-based fMRI data, in this study we use rs-fMRI data. Numerous studies have been conducted on ASD subjects using rs-fMRI data in the recent decade. According to these studies, abnormal functional/effective connectivity between brain areas has been reported in ASD subjects. Most studies on functional or effective connectivity of ASD individuals corroborate the underconnectivity theory in ASD which is based on the long-range underconnectivity and sometimes short-range overconnectivity. According to the underconnectivity theory in ASD, different areas of the brain are not

properly connected to each other and this causes them to function asynchronously and uncoordinated [5]. Since ASD affects brain functional and effective connectivities, we have extracted features based on the functional and effective connectivities to classify ASD subjects from healthy individuals. Deep learning is a field of machine learning in which the features are automatically extracted from data. Unlike conventional artificial neural networks, which are shallow feature learning methods, deep learning methods employ multiple deep layers of perceptrons that capture both low-level and high-level representations of data, enabling them to learn richer abstractions of inputs. This obviates the need for manual engineering of features and allows deep learning models to naturally uncover previously unknown patterns and generalize better to new data [6]. We will extract low-level features of brain functional and effective connectivities and subsequently the high-level features are extracted using a stacked autoencoder neural network. Finally, we will classify the extracted high-level features by using a Multi-Layered Perceptron (MLP) neural network.

1.1. Related Works

We briefly review some recent studies on ASD diagnosis using rs-fMRI data and deep learning methods in the recent three years (after 2020) in this section. Some previous studies that have used deep neural networks for diagnosing ASD using rs-fMRI are depicted in Table 1.

Our main question in this paper is whether we can diagnose ASD using effective connectivity measures and stacked autoencoder which is a type of deep neural networks? If the answer is positive, will our results improve compared to functional connectivity measures or not?

The purpose of this paper is to diagnose ASD using effective connectivity measures, stacked autoencoder, and rs-fMRI data, and to compare its results with those obtained using functional connectivity measures. As far as we know, this is the first time that Granger Causality (GC) and stacked autoencoder have been used to diagnose ASD together.

Table 1. Some previous studies that used deep neural networks for diagnosing ASD using rs-fMRI

| Reference | The number of subjects | Features | Classification | Accuracy% | Sensitivity% | Specificity% |
|-----------|--|---|--|----------------------------|--------------|----------------------------------|
| [7] | ABIDE I 403 ASD 468 TC | 116 regions Automated Anatomical Labeling atlas Pearson Correlation Coefficient (PCC) | Fully Connected Neural Network (FCNN) | 69.81% | 63.05% | 75.63% |
| [8] | ABIDE GU 51 ASD 55 TC NYU 48 ASD 30 TC | Fusion of functional connectivity (FC) And amplitude of low frequency fluctuation (ALFF) | Convolutional Neural network (CNN) | 68.54% | 69.49% | 67.58% |
| [9] | ABIDE 403 ASD 468 TC | construction of the brain networks from brain fMRI images, and defining the raw features based on such brain networks, and employing an AE to learn the advanced features from the raw features | DNN | 76.2% | — | — |
| [10] | ABIDE 505 ASD 530 TC | 200 regions Craddock 200 PCC Sparse Autoencoder is used for feature reduction | Two hidden layers deep-neural networks with Softmax function as output layer | 70.8% | 62.2% | 79.1% |
| [11] | ABIDE 432 ASD 556 TC | 200 regions Craddock 200 PCC | ANN Random Forest Autoencoders | 65.99% | 71.35% | 0.595 0.806 |
| [12] | ABIDE I 403 ASD 468 TC | 264 regions PCC | semi-supervised autoencoder | 60.93% | 60.63% | 0.247 0.245 0.890 0.886 |
| [13] | ABIDE 505 ASD 530 TC | 200 regions Craddock 200 PCC F-score | Autoencoder and Single Layer Perceptron (SLP) | 67.61 | 69.93% | 0.787 0.750 0.532 0.634 |
| [14] | ABIDE I 505 ASD 530 TC | 392 regions Craddock 400 PCC | a deep learning model with two procedures – simplified VAE pretraining and MLP fine-tuning | 87.2% | 89.9% | 80.3% |
| [15] | ABIDE 505 ASD 530 TC | 400 regions CC400 PCC | generalized end-to-end CNN, a deep learning (DL)-based model referred to as ASDC-Net. | average accuracy 64.53% | — | — |
| | | | | 78.12% | 77.88% | 78.34% |
| | | | | 76.72% | 76.68% | 76.79% |

2. Materials and Methods

The proposed approach is introduced in this section. This approach consists of data acquisition, data preprocessing, brain parcellation using the Harvard-Oxford (HO) atlas, feature extraction, feature reduction, and finally classification. The block diagram of this study is depicted in Figure 1.

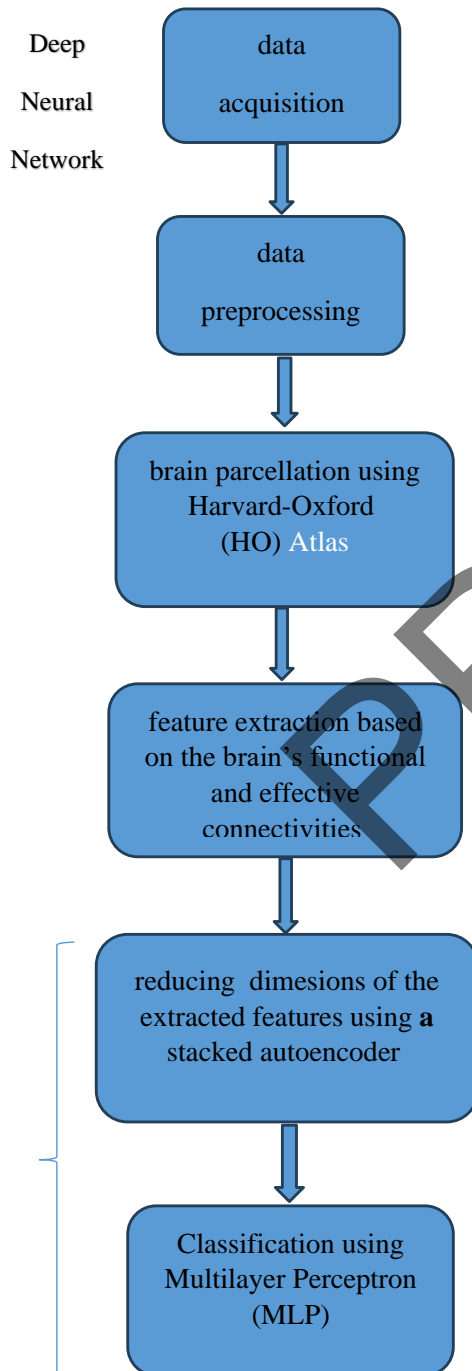


Figure 1. The block diagram of this study

2.1. Data Acquisition

The Autism Brain Imaging Data Exchange (ABIDE I) provided ASD brain imaging data. ABIDE I contains 17 international sites that share rs-fMRI data. It contains 1112 subjects which are composed of 539 ASD subjects and 573 healthy individuals. This dataset has been acquired from people between ages 7 and 64 years and was published in August 2012. We conducted our analyses on a publicly accessible, preprocessed version of this dataset provided by the Preprocessed Connectome Project initiative. Specifically, we used the data processed with the Configurable Pipeline for the Analysis of Connectomes (C-PAC). The data were chosen based on quality visual inspection results by three human experts who checked for incomplete brain coverage, high movement peaks, ghosting, and other scanner artifacts. This resulted in 871 subjects from the initial 1112. These 871 data include 403 data samples of ASD people and 468 data samples of healthy people. We explored pipelines that extract neurophenotypes from aggregate rs-fMRI datasets.

You can freely access the above data using the http://fcon_1000.projects.nitrc.org/indi/abide/ link to see the full details of the ABIDE I dataset.

2.2. Data Preprocessing:

The preprocessed rs-fMRI data using the C-PAC pipeline has been downloaded from <http://preprocessed-connectomes-project.org/abide/cpac.html>

2.3. Preprocessing with CPAC

Preprocessing of the ABIDE data was done with version X of the Configurable Pipeline for the Analysis of Connectomes (C-PAC, <http://fcp-indi.github.com>). This Python-based pipeline tool makes use of AFNI, ANTs, FSL, and custom Python code. Below, some of the structural and functional preprocessing steps are explained:

2.4. Structural Preprocessing

1. Skull-stripping by using AFNI's 3dSkullStrip tool

2. Parcellating the brain into three tissue types by using FSL's FAST
3. Restricting the segmentation of individual tissues by using tissue priors from the standard space provided by using FSL
4. Normalizing individual skull-stripped brains to Montreal Neurological Institute (MNI)152 stereotactic space (1 mm³ isotropic) by using linear and non-linear registration methods by ANTs.

2.5. Functional Preprocessing

1. Slice timing correction by using AFNI's 3dTshift
2. Motion correction to the average image by using AFNI's 3dvolreg (two iterations)
3. Skull-stripping by using AFNI's 3dAutomask
4. Normalizing global mean intensity to 10,000
5. Applying nuisance signal regression
6. Applying band-pass filter (0.01-0.1Hz)

2.6. Classification using Functional Connectivity

2.6.1. Low-Level Feature Extraction by Calculating the PCC

The functional magnetic resonance imaging technique records three-dimensional T_2^* weighted images of the whole brain in short time intervals of T_R . If we consider the volume unit called voxel as a sample in these consecutive three-dimensional images, according to the neural activity in the area where the desired voxel is located, the intensity of the blood flow and the amount of oxygen in the blood will change, and the desired voxel will have different intensity at different times. If we model the intensity of a voxel as a signal, we will have a time series that is called the blood-oxygen-level-dependent (BOLD) signal of that voxel which is shown in Figure 2.

Brain parcellation was done using the Harvard-Oxford (HO) atlas in FSL software. This atlas includes 96 cortical regions and 16 subcortical regions, so it includes a total of 112 brain regions.

Each voxel has different intensities in the imaging sequence of the total brain volume due to the changes in the neural activities in that voxel; thus, each voxel will have a BOLD time series. Since each brain region comprises a large number of voxels, each brain region has a large number of time series. If we average all the time series of the voxels of each region, each region will have one time series. For low-level feature extraction, the relationship between these time series is calculated by two different methods. Since Pearson correlation coefficient (PCC) is the most widely used functional connectivity measure of fMRI data, the first method is to calculate the PCC between the time series of one region and the average time series of other regions and the second method is to calculate the Granger Causality (GC) as the most widely used effective connectivity measure.

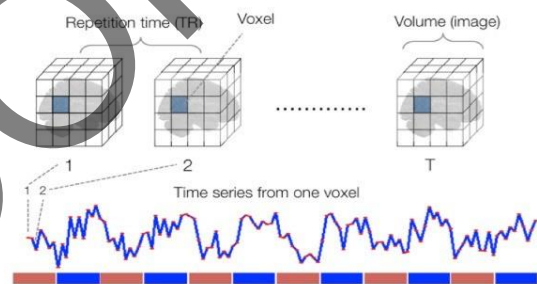


Figure 2. BOLD time series resulting from the neural activity corresponding to one voxel [16]

The brain is parcellated to 112 regions using the Harvard-Oxford (HO) atlas. Because in some subjects and some of these 112 regions the total value of the time series is zero, the PCC value is not defined. We ignore all of these regions which are a total of 12 regions to solve the problem. Since there are 100 brain regions for each subject, computing all pairwise correlations generates a correlation matrix $M_{100 \times 100}$. Because this matrix is symmetric, 4950 unrepeated features are obtained. Since we examine 870 subjects in this study, we have a representation vector with dimensions of 4950×870 , which is the input of the stacked autoencoder.

2.6.2. High-Level Feature Extraction and Classification

High-level feature extraction is performed using a stacked autoencoder neural network and classification is done using a Multi-Layered Perceptron (MLP) neural network. Various methods have been used for feature extraction and supervised selection of the feature in various studies as mentioned in the related works section, and in all mentioned references using different methods to extract and reduce the dimension of feature space are strengthened and less effective features are removed; therefore, in addition to reducing the amount of calculations, the performance of classification methods is improved. However, supervised selection of the features from the feature space avoids exploration of new discriminative patterns. Deep learning explores complex structures in huge databases. Deep learning methods can learn features hierarchically. In this process, the features of each level are made from the combination of the features at their lower level that leads to features learning at different levels of abstraction which helps the system to learn complex functions. These functions convert inputs to outputs directly and by passing through this chain.

We have a representation vector with dimensions of 4950×870 as mentioned before, which is the input of the neural network. In order to design the neural network, we use a stacked autoencoder consisting of seven autoencoders and an MLP network with two hidden layers as a classifier. We extract the linear and non-linear relationships of the obtained features using a stacked autoencoder deep neural network and reduce the dimension using the compression capability of the autoencoders, simultaneously.

Figure 3 shows a general diagram of the use of a stacked autoencoder and MLP classifier. The data set was divided into training, validation, and test sets, which contained 70%, 15%, and 15% of data, respectively. The number of neurons in the encoder layer in the first, second, third, fourth, fifth, sixth, and seventh auto-encoder is 4700, 4000, 2000, 1000, 500, 200, and 100, respectively. The number of neurons in the encoder layer and the number of autoencoders are obtained by trial and error. Using trial and error is due to the different nature of the different datasets because each dataset has its own properties and there is not a

standard method to determine the optimal number of hidden layers, and the number of neurons in these layers.

Regarding the MLP neural network structure, the number of neurons in the first and second hidden layers is 60 and 30, respectively. The number of neurons in the output layer is two. The activation function of the MLP neural network and the autoencoder neural network is the softsign function, which has a linear region, a non-linear region, a positive region, and a negative region.

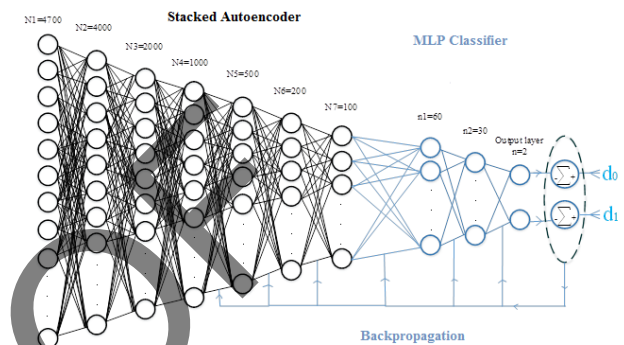


Figure 3. General diagram of the proposed network

Seven autoencoders are used to reduce the dimension and extract high-level features as can be seen from Figure 3. First, the weights are selected randomly in all autoencoders, and then they are trained. The desired output in the first autoencoder is the input vector X (low-level features); therefore, we compare the output with the input and form the reconstruction error. The weights of this autoencoder are trained through the back-propagation method of the reconstruction error.

The main part of an autoencoder is the middle hidden layer (encoder layer) which has 4700 neurons in the first autoencoder. This middle layer is the input of the next autoencoder, whose weights are trained similarly. This process continues until the seventh autoencoder. All these seven autoencoders are trained in an unsupervised manner using the back-propagation method of the reconstruction error, and their weights are adjusted. Finally, the neurons of the middle layer of the seventh autoencoder, which has 100 neurons, are given to the MLP network as the extracted high-level features. The MLP network consists of two hidden layers. The learning in the MLP network, unlike autoencoders, is supervised. The training of the weights of the MLP is done using the error

backpropagation method. When the output is compared with the desired value in the last layer and the error is returned back using the backpropagation method, it not only trains the MLP's weights but also adjusts the weights of up to three layers of the previous autoencoder. The reason why it does not go further is that the value of the derivative of the error is very small and the weights of other layers are not updated.

2.7. Classification using Effective Connectivity

2.7.1. Low-level Feature Extraction by Calculating the Granger Causality (GC)

Low-level feature extraction is done by calculating the GC between each pair of time series (brain region). GC is a tool to estimate effective linear relationships between two variables. GC is used to analyze the flow of information between time series.

The brain parcellation using the Harvard-Oxford (HO) atlas created 100 regions. If we want to calculate the GC between each pair of time series (brain region), we will have a 100×100 G matrix which is not symmetrical; therefore, we have a representation vector with dimensions of 9900×870 . Since the number of features is very large, we try to reduce the dimensions of the features to $9900/2=4450$ for reducing the computational cost. Since the value of g_{ij} is different from the value of g_{ji} in the GC matrix. We obtain the ratio of the difference of g_{ij} and g_{ji} to their sum according to Equation 1:

$$g_d = \frac{g_{ij} - g_{ji}}{g_{ij} + g_{ji}} \quad (1)$$

The sign of g_d shows the dominant direction of information flow between the i^{th} and j^{th} brain regions. Using g_d instead of g_{ij} and g_{ji} , the number of features of the Granger causality matrix is halved and will be the same as the number of features of the correlation coefficient matrix.

2.7.2. High-Level Feature Extraction and Classification:

High-level feature extraction is performed using a stacked autoencoder and classification is performed using a Multi-Layered Perceptron (MLP) neural

network in this section. The number of the autoencoders in the stacked autoencoder is 7. The number of neurons in the encoder layer in the first, second, third, fourth, fifth, sixth, and seventh autoencoder are 4700, 4000, 2000, 1000, 500, 200, and 100, respectively. The number of hidden layers in the MLP neural network is 2. The number of neurons in the first and second hidden layers is 50 and 25, respectively. The number of neurons in the output layer is 2.

3. Results

3.1. Results of Classification using Functional Connectivity

Here, the reported results are related to low-level feature extraction by calculating the Pearson Correlation Coefficient (PCC) and high-level feature extraction using a stacked autoencoder neural network and classification using a Multi-Layered Perceptron (MLP) neural network. These results are shown in the form of a diagram of reconstruction error of training and validation data in autoencoders, in the form of input and output (reconstructed input) in autoencoders.

Figures 4a, 4b, 4c, 4d, 4e, 4f, and 4g show the diagram of reconstruction error of training and validation data in the first, second, third, fourth, fifth, sixth, and seventh autoencoders, respectively. When the reconstruction error of the training and validation data in each autoencoder is minimized and the input and output diagrams almost coincide, we stop training the autoencoders.

The dimensions of the autoencoder's input in the first, second, third, fourth, fifth, sixth, and seventh autoencoders, are 870×4950 , 870×4700 , 870×4000 , 870×2000 , 870×1000 , 870×500 , and 870×200 , respectively. The number of neurons in the encoder layer in the first, second, third, fourth, fifth, sixth, and seventh autoencoders are 4700, 4000, 2000, 1000, 500, 200, and 100, respectively. Due to the small number of representation vectors and to prevent overfitting, validation error have a direct relationship with the sum of the weights, the diagrams of this stage have fluctuated. The dropout rate or α and the training rate or η in the first, second, third, fourth, fifth,

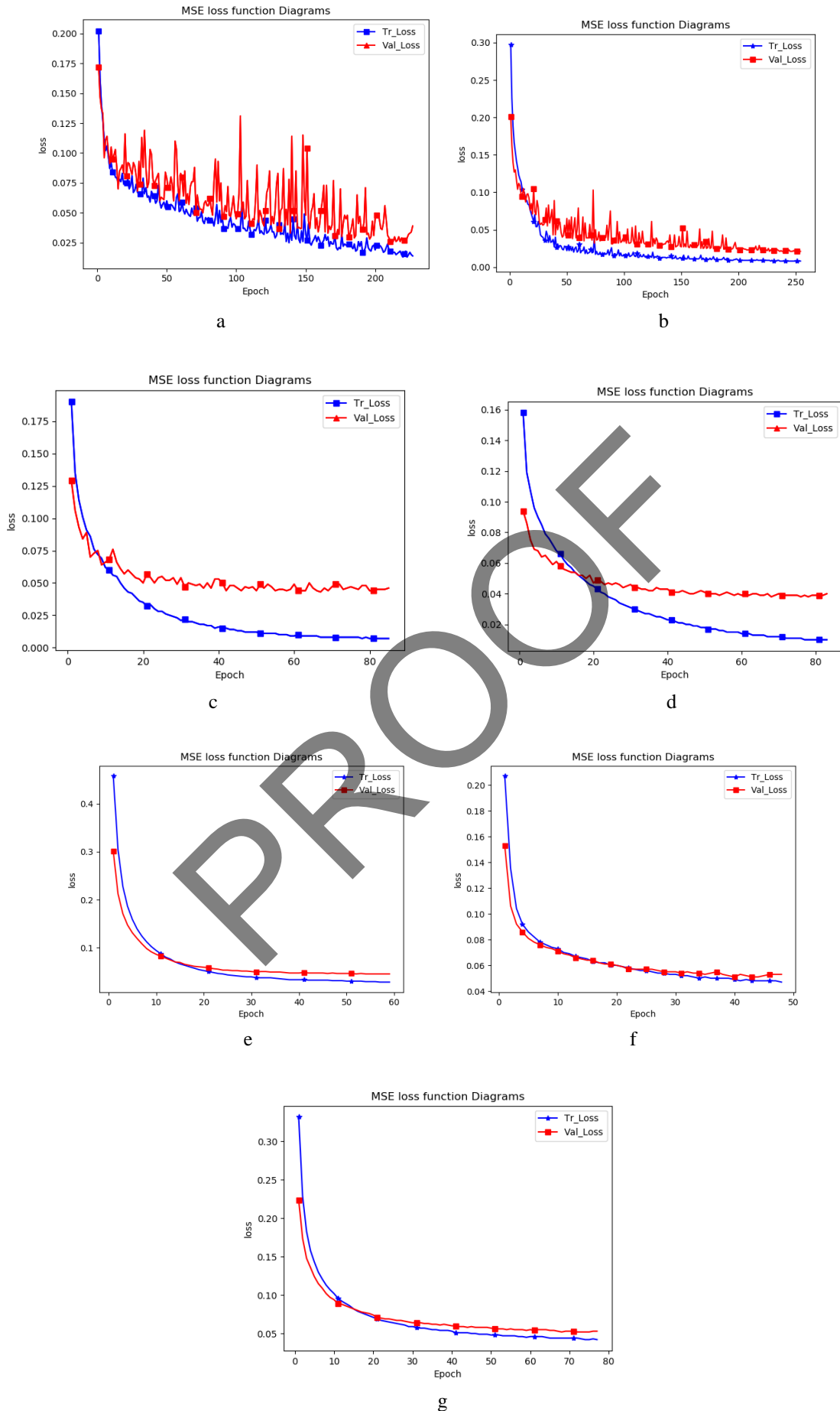


Figure 4. Training and validation errors in the first, second, third, fourth, fifth, sixth, and seventh autoencoders in stacked autoencoder are shown in Figures a, b, c, d, e, f, and g, respectively

$\eta=0.001$), ($\alpha=0.1, \eta=0.001$), ($\alpha=0.05, \eta=0.001$), ($\alpha=0, \eta=0.005$), ($\alpha=0.1, \eta=0.01$), ($\alpha=0.1, \eta=0.01$), and ($\alpha=0, \eta=0.05$), respectively.

Results of classification using functional connectivity are reported in Table 2.

Table 2. Results of classification using functional connectivity

| | Accuracy | Sensitivity | specificity |
|-----------------------|----------|-------------|-------------|
| Results for test data | 67.8% | 68.5% | 66.6% |

3.2. Results of Classification using Effective Connectivity

Here, the reported results are related to low-level feature extraction by calculating the Granger Causality (GC) using model order 1, high-level feature extraction using a stacked autoencoder neural network, and classification using a multilayer perceptron neural network. These results are shown in the form of a diagram of reconstruction error of training and validation data in autoencoders, in the form of input and output (reconstructed input) in autoencoders.

Figures 5h, 5i, 5j, 5k, 5l, 5m, and 5n show the diagram of training and validation error in the first, second, third, fourth, fifth, sixth, and seventh autoencoders, respectively.

The dimensions of the autoencoder's input in the first, second, third, fourth, fifth, sixth, and seventh autoencoders are 870×4950 , 870×4700 , 870×4000 , 870×2000 , 870×1000 , 870×500 , and 870×200 , respectively. The number of neurons in the encoder layer in the first, second, third, fourth, fifth, sixth, and seventh autoencoders, are 4700, 4000, 2000, 1000, 500, 200, and 100, respectively. The dropout rate or α and the training rate or η in the first, second, third, fourth, fifth, sixth, and seventh autoencoders are ($\alpha=0.2, \eta=0.001$), ($\alpha=0.1, \eta=0.001$), ($\alpha=0.1, \eta=0.005$), ($\alpha=0.1, \eta=0.01$), ($\alpha=0.1, \eta=0.01$), ($\alpha=0, \eta=0.05$), and ($\alpha=0, \eta=0.02$), respectively.

Results of classification using effective connectivity are reported in Table 3.

Table 3. Results of classification using effective connectivity

| | Accuracy | Sensitivity | specificity |
|-----------------------|----------|-------------|-------------|
| Results for test data | 67.6% | 73.1% | 60.8% |

4. Discussion

We implemented diagnosing ASD using rs-fMRI data and features based on (functional and effective) brain connectivities and deep autoencoders in this paper. When we used functional connectivity features for ASD diagnosis, low-level feature extraction was done by calculating the Pearson Correlation Coefficient (PCC), and high-level feature extraction was performed using a stacked autoencoder and classification was done using a multi-layered perceptron (MLP) neural which achieved an accuracy of 67.8%, sensitivity of 68.5%, and specificity of 66.6%. When we used effective connectivity features for ASD diagnosis, low-level feature extraction was done by calculating the Granger Causality (GC) with model order one and the next steps were the same as those for functional connectivity features which achieved an accuracy of 67.6%, sensitivity of 71.3%, and specificity of 60.8%. Although in some previous studies, diagnosing ASD has been done using functional brain connectivity and autoencoders, it has not been done using effective brain connectivity and autoencoders; therefore, in this study for the first time, diagnosing ASD has been done by extracting brain-effective connectivity features by calculating the GC, reducing feature space using an autoencoder, and performing the classification using an MLP. Comparing the obtained results, although the classification accuracy using functional and effective connectivity was almost similar, the sensitivity using effective connectivity was notably higher than that obtained using functional connectivity. Since sensitivity is more important in medical diagnosis, these results are remarkable. If the patient is wrongly classified as healthy, the rehabilitation and treatment process of the patient will not be done, and the patient's golden time for treatment may be lost. If a healthy person is wrongly diagnosed as a patient, after

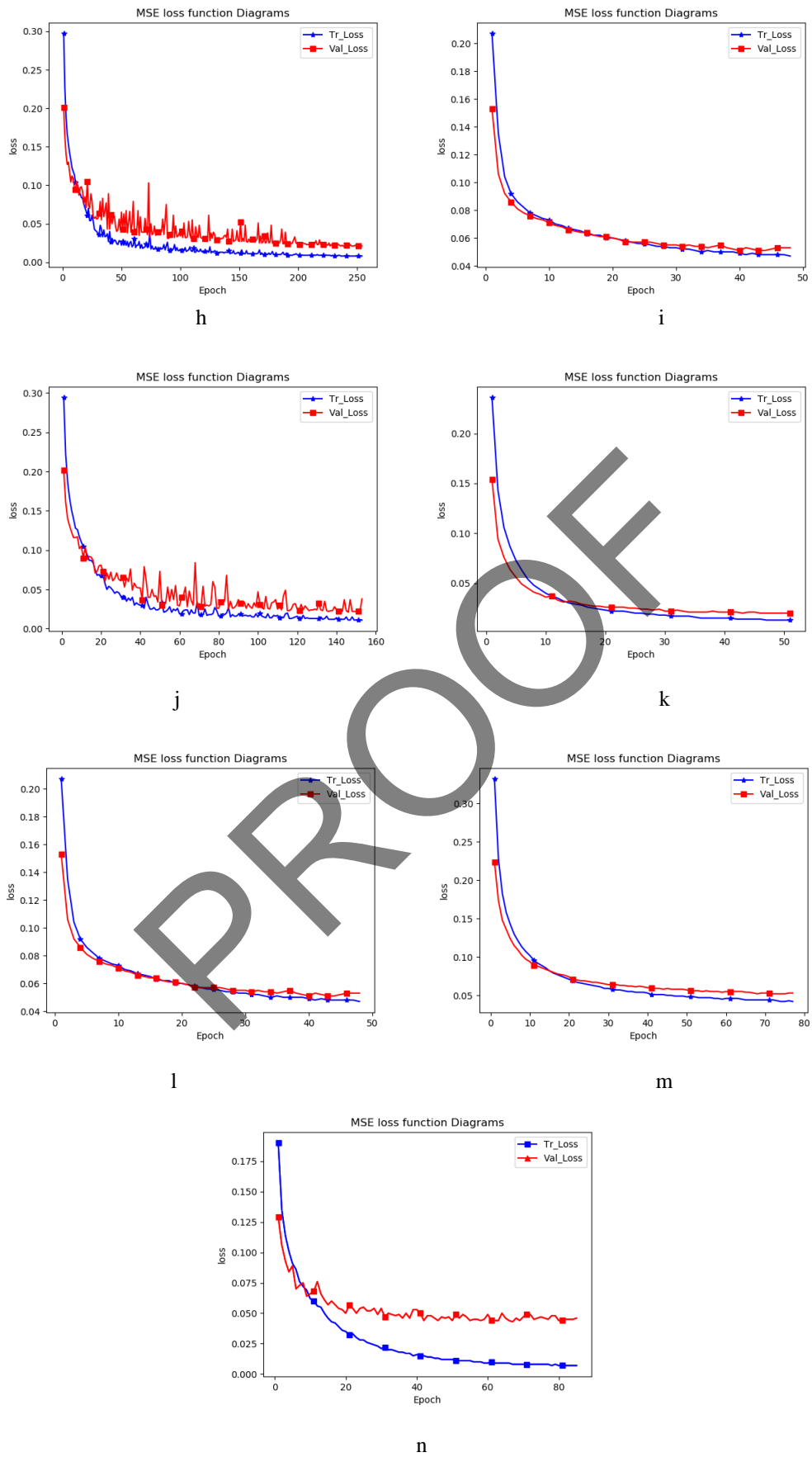


Figure 5. Training and validation errors in the first, second, third, fourth, fifth, sixth, and seventh autoencoders in a stacked autoencoder are shown in Figures h, i, j, k, l, m, and n, respectively

more complete diagnostic procedures, he will be diagnosed as healthy.

Since the obtained sensitivity using effective connectivity was higher than that obtained using functional connectivity, and considering that in diagnosing ASD, sensitivity is more important than specificity, using effective connectivity may be preferable to using functional connectivity for ASD diagnosis. This may be because the direction of information flow is considered in effective connectivity but this is not the case for functional connectivity. In fact, ASD may distort the direction of some brain information flows which cannot be detected using the functional connectivity measures.

In this section, we compare the results of some similar studies reported in Table 1 with the results of our study.

In [7], Hu *et al.* conducted their analysis on the same data that we have used in our paper. Although the accuracy achieved by their method is slightly higher than that by our method, the sensitivity obtained by our method is significantly higher than the sensitivity obtained by their method. Since sensitivity is more important in medical diagnosis, overall, the results of our study are more favorable compared to theirs.

In [8], You *et al.* analyzed the data of 184 subjects from the ABIDE dataset. The number of subjects in their study is significantly less than ours; however, the accuracy achieved in our paper is close to the accuracy achieved in their paper, and the sensitivity obtained using effective connectivity in our study is higher than theirs.

In [10], Almuqhim and Saeed analyzed the data of 1035 subjects from the ABIDE dataset. Although the accuracy achieved in their study is slightly higher than ours, the sensitivity obtained in their study is significantly lower than ours.

In [11], Ingalthalika *et al.* analyzed the data of 988 subjects from the ABIDE dataset. The accuracy obtained in their method is almost equal to ours. The sensitivity achieved in their method is higher than ours, but their specificity is significantly lower than ours. Consequently, low specificity reduces the credibility of their results.

In [13], Zhang *et al.* analyzed the data of 1035 subjects from the ABIDE dataset. Although the number of subjects in their study is higher than ours, their accuracy is lower than ours.

The limitations of our method are categorized as follows:

1- Our method isn't practical yet because it needs more experiments before it can be used in the clinic. It should be trained on larger data to generalize to new people and lead to higher accuracy levels. Also, to make this method more practical, early diagnosis should be considered. Although the ABIDE data is large compared to most fMRI datasets, it is still not much for deep neural networks. Since deep neural networks need a lot of data to be trained well, larger datasets should become available. The data augmentation methods or transfer learning also be used to lead to better results. Synthetic data can be generated using Generative Adversarial Network (GAN) and added to the training data. Methods that enable learning from very limited labeled data can be used, such as one-shot learning.

2- The Golden standard age for diagnosing ASD is under 3 years old, so a dataset should be recorded from children under 3 years old to let us design a computer-aided diagnosis system for early diagnosis. It is very difficult to record fMRI data from children under 3 years old, and we do not have access to such data now. Because the age range of the used dataset in this study is reported from 7 to 64 years old, the used dataset is not suitable for early diagnosis. The method of this study can have a favorable result on the obtained data and on the same specifications. If the age range is much higher or lower than the age range of 7 to 64 years, the desired result may not be achieved.

3- Since gender affects the symptoms of ASD in the brain and the brain disorders of an autistic female may be different from those of an autistic male, the biomarkers of ASD may be gender-dependent. The number of autistic females is less than the number of autistic males and in ASD there is a 4:1 male-to-female prevalence rate. Since the female gender is much less than the male gender in the ABIDE dataset, this dataset is actually more suitable for diagnosing ASD in males. To get accurate results, we have to take data from a large number of females and a large number of males and we have to train the classifier on

the data of each gender separately; therefore, the results are expected to be better than when the classifier is trained on the entire data of both genders. By doing this, we will have a sex-dependent diagnosis system for ASD.

4- Because PCC and GC are both linear criteria, they can only detect linear connectivities. If ASD leads to dissonances in non-linear connectivities, these dissonances may not be visible in the matrix of linear connectivities and some valuable diagnostic information may be lost.

Some suggestions for future studies are as follows:
1- In Table 1, [12], [14], and [15] have achieved high results in diagnosing ASD using functional brain connectivity and deep neural networks. Because in our method, the achieved sensitivity using effective connectivity is notably higher than the achieved sensitivity using functional connectivity for ASD diagnosis, it is suggested to investigate the use of effective connectivity instead of functional connectivity in the methods of [12], [14], and [15].

2- It is suggested to provide a computer-aided diagnosis (CAD) system that can diagnose ASD in different age groups and gender groups of this data set.

3- More complex functional and effective connectivity measures can be used to extract more complex connectivity features, for example, criteria that measure non-linear or multivariate connectivities can be used.

4- Various classifiers can be applied to the output of the autoencoder instead of MLP

5- Functional brain atlases can be used instead of structural ones.

6- Different types of deep neural networks can be used instead of autoencoder.

5. Conclusion

When we used functional connectivity for Autism Spectrum Disorder (ASD) diagnosis using a stacked autoencoder and a multi-layered perceptron (MLP) classifier, we achieved an accuracy of 67.8%, sensitivity of 68.5%, and specificity of 66.6%, and in classification using effective connectivity, we achieved an accuracy of 67.6%, sensitivity of 71.3%, and specificity of 60.8%. Considering the main

objective of this paper, which is to evaluate the feasibility of using effective connectivity measures and a stacked autoencoder in the diagnosis of ASD by rs-fMRI data and to compare the results with functional connectivity measures, the results obtained using effective connectivity in our study were better than the results obtained using functional connectivity in many studies. In some studies that had better results in terms of accuracy and sensitivity, they used a larger feature space as input for deep neural networks; in other words, they conducted their analysis with atlases that had more brain regions. Nonetheless, their results were slightly better than ours. Our findings indicate that although the accuracy obtained using functional and effective connectivity are almost similar, the sensitivity is notably higher using effective connectivity. Since sensitivity is more important than specificity in the medical diagnosis, it seems that using effective connectivity features may outperform the ASD diagnosis in practice.

In [7], Hu *et al.* conducted their analysis on the same data that we have used in our paper. Although the accuracy achieved by their method is slightly higher than that by our method, the sensitivity obtained by our method is significantly higher than the sensitivity obtained by their method. Since sensitivity is more important in medical diagnosis, overall, the results of our study are more favorable compared to theirs.

In [8], You *et al.* analyzed the data of 184 subjects from the ABIDE dataset. The number of subjects in their study is significantly less than ours; however, the accuracy achieved in our paper is close to the accuracy achieved in their paper, and the sensitivity obtained using effective connectivity in our study is higher than theirs.

In [10], Almuqhim and Saeed analyzed the data of 1035 subjects from the ABIDE dataset. Although the accuracy achieved in their study is slightly higher than ours, the sensitivity obtained in their study is significantly lower than ours.

In [11], Ingalhalikar *et al.* analyzed the data of 988 subjects from the ABIDE dataset. The accuracy obtained in their method is almost equal to ours. The sensitivity achieved in their method is higher than ours, but their specificity is significantly lower than

ours. Consequently, low specificity reduces the credibility of their results.

In [13], Zhang *et al.* analyzed the data of 1035 subjects from the ABIDE dataset. Although the number of subjects in their study is higher than ours, their accuracy is lower than ours.

The number of brain regions in the atlas which has been used in the [14] and [15] is four times greater than the number of brain regions in the atlas used in our paper, thus the aforementioned studies have provided more rich information as input to the neural network. Additionally, the number of subjects in [14] and [15] is 16% higher than the number of subjects in our paper. These factors may have led to the results of these studies being better in terms of accuracy compared to the results of our paper. The results of [14] and [15] have been slightly improved in terms of sensitivity compared to the results of our paper. If we apply our method to the atlas used in the [14] and [15] with the same number of brain regions, we can then compare our results with theirs. However, in the current format, an accurate quantitative comparison between our method and their methods is not possible. A quantitative comparison of our method with the methods in [14] and [15] is only possible if we reimplement and evaluate our method using the atlas from those papers. In the current format, this comparison is not reliable.

Diagnosing ASD has not been done using effective brain connectivity and autoencoder before. In this study, diagnosing ASD has been done using effective brain connectivity by calculating the Granger Causality (GC), autoencoder for feature reduction, and MLP as a classifier.

In this section, we aim to explain the merits of using Granger Causality (GC) and stacked autoencoder together. For diagnosing ASD using rs-fMRI, the correlation coefficient, which is a measure of functional connectivity, has often been used in past studies. Effective connectivity measures, such as Granger causality have been rarely used in this field. Since effective connectivity measures quantify information flow, they provide distinct information compared to functional connectivity measures. In fact, although the correlation coefficient is an undirected connectivity measure, Granger causality is a directed one. In addition, an autoencoder is a filter-based

nonlinear dimension reduction method that can compress the feature space nonlinearly, allowing for the reconstruction of the feature space from the compressed features. Consequently, the simultaneous use of these two tools enables the utilization of information flow between brain regions for the diagnosis of ASD.

Some suggestions for future studies are as follows:

- 1- Increasing the amount of data
- 2- Providing a Computer-Aided Diagnosis (CAD) system for diagnosing ASD across different age and gender groups
- 3- Using more complex functional and effective connectivity measures to extract advanced connectivity features
- 4- Applying and comparing various classifiers on the output of autoencoder instead of MLP
- 5- Utilizing functional brain atlases instead of structural ones
- 6- Implementing different types of deep neural networks instead of autoencoder.

References

- 1- O. Dekhil, H. Hajjdiab, A. Shalaby, M. T. Ali, B. Ayinde, A. Switala, A. Elshamekh, M. Ghazal, R. Keynton, and G. Barnes, "Using resting state functional MRI to build a personalized autism diagnosis system," *PLoS one*, vol. 13, no. 10, p. e0206351, (2018).
- 2- N. Salari, S. Rasoulpoor, S. Rasoulpoor, S. Shohaim <https://doi.org/10.1089/cmb.2020.0252i>, S. Jafarpour, N. Abdoli, B. Khaledi-Paveh, and M. Mohammadi, "The global prevalence of autism spectrum disorder: a comprehensive systematic review and meta-analysis," *Italian Journal of Pediatrics*, vol. 48, no. 1, pp. 1-16, (2022).
- 3- H. Choi, "Functional connectivity patterns of autism spectrum disorder identified by deep feature learning," *arXiv preprint arXiv:1707.07932*, (2017).
- 4- M. Daliri and M. Behroozi, "Advantages and disadvantages of resting state functional connectivity magnetic resonance imaging for clinical applications," *OMICS Journal of Radiology*, vol. 3, no. 1, pp. 1-2, (2013).
- 5- A. Khadem, G.-A. Hossein-Zadeh, and A. Khorrami, "Long-range reduced predictive information transfers of autistic youths in EEG sensor-space during face processing," *Brain topography*, vol. 29, pp. 283-295, (2016).

- 6- A. A.-A. Valliani, D. Ranti, and E. K. Oermann, "Deep learning and neurology: a systematic review," *Neurology and therapy*, vol. 8, pp. 351-365, (2019).
- 7- J. Hu, L. Cao, T. Li, B. Liao, S. Dong, and P. Li, "Interpretable learning approaches in resting-state functional connectivity analysis: the case of autism spectrum disorder," *Computational and mathematical methods in medicine*, vol. 2020, (2020).
- 8- Y. You, H. Liu, S. Zhang, and L. Shao, "Classification of autism based on fMRI data with feature-fused convolutional neural network," in *Cyberspace Data and Intelligence, and Cyber-Living, Syndrome, and Health: International 2020 Cyberspace Congress, CyberDI/CyberLife 2020, Beijing, China, December 10–12, 2020, Proceedings 4*, 2020: Springer, pp. 77-88.
- 9- W. Yin, S. Mostafa, and F.-X. Wu, "Diagnosis of autism spectrum disorder based on functional brain networks with deep learning," *Journal of Computational Biology*, vol. 28, no. 2, pp. 146-165, (2021).
- 10- F. Almuqhim and F. Saeed, "ASD-SAENet: a sparse autoencoder, and deep-neural network model for detecting autism spectrum disorder (ASD) using fMRI data," *Frontiers in Computational Neuroscience*, vol. 15, p. 654315, (2021).
- 11- M. Ingahalikar, S. Shinde, A. Karmarkar, A. Rajan, D. Rangaprakash, and G. Deshpande, "Functional connectivity-based prediction of Autism on site harmonized ABIDE dataset," *IEEE Transactions on Biomedical Engineering*, vol. 68, no. 12, pp. 3628-3637, (2021).
- 12- W. Yin, L. Li, and F.-X. Wu, "A semi-supervised autoencoder for autism disease diagnosis," *Neurocomputing*, vol. 483, pp. 140-147, (2022).
- 13- J. Zhang, F. Feng, T. Han, X. Gong, and F. Duan, "Detection of autism spectrum disorder using fMRI functional connectivity with feature selection and deep learning," *Cognitive Computation*, vol. 15, no. 4, pp. 1106-1117, (2023).
- 14- F. Zhang, Y. Wei, J. Liu, Y. Wang, W. Xi, and Y. Pan, "Identification of Autism spectrum disorder based on a novel feature selection method and Variational Autoencoder," *Computers in Biology and Medicine*, vol. 148, p. 105854, (2022).
- 15- A. Chandra, S. Verma, A. S. Raghuvanshi, and N. K. Bodhey, "ASDC-Net: Optimized Convolutional Neural Network-Based Automatic Autism Spectrum Disorder Classification Using rs-fMRI Data," *IETE Journal of Research*, pp. 1-14, (2023).
- 16- W. a. M. Yin, Sakib and Wu, Fang-Xiang, "Diagnosis of autism spectrum disorder based on functional brain networks with deep learning," *Journal of Computational Biology*, vol. 28, pp. 146-165, (2021).